European Heart Journal – Cardiovascular Imaging (2015) **16**, 910–918
doi:10.1093/ehjci/jev018

Simultaneous morphological and biochemical endogenous optical imaging of atherosclerosis

Javier A. Jo[1]*, Jesung Park[1], Paritosh Pande[1], Sebina Shrestha[1], Michael J. Serafino[1], J. de Jesus Rico Jimenez[1], Fred Clubb[1,2], Brian Walton[3], L. Maximilian Buja[4], Jennifer E. Phipps[5], Marc D. Feldman[5], Jessie Adame[6], and Brian E. Applegate[1]

[1]Department of Biomedical Engineering, Texas A&M University, 5062 Emerging Technologies Building, 3120 TAMU, College Station, TX 77843-3120, USA; [2]Department of Veterinary Pathobiology, Texas A&M University, College Station, TX, USA; [3]Department of Cardiology, Texas Heart Institute at St. Luke's Episcopal Hospital, Houston, TX, USA; [4]Department of Cardiovascular Pathology Research, Texas Heart Institute at St. Luke's Episcopal Hospital, Houston, TX, USA; [5]University of Texas Health Science Center San Antonio, San Antonio, TX, USA; and [6]Autopsy and Pathology Services, Houston, TX, USA

Received 23 October 2014; accepted after revision 26 January 2015; online publish-ahead-of-print 26 February 2015

Aims The aim of this study was to validate novel imaging technology for simultaneous morphological and biochemical endogenous optical imaging of coronary atherosclerotic plaque.

Methods and results Optical coherence tomography (OCT) generates high-resolution 3D images of plaque morphology and endogenous fluorescence lifetime imaging microscopy (FLIM) characterizes biochemical composition. Both imaging modalities rely on plaque's intrinsic optical characteristics, making contrast agents unnecessary. A multimodal OCT/FLIM system was utilized to generate luminal biochemical maps superimposed on high-resolution (7 μm axial and 13 μm lateral) structural volumetric images. Forty-seven fresh postmortem human coronary segments were imaged: pathological intimal thickening (PIT, $n = 26$), fibroatheroma (FA, $n = 12$), thin-cap FA (TCFA, $n = 2$), and fibrocalcific plaque (CA, $n = 7$), determined by histopathology. Multimodal images were evaluated, and each plaque identified as PIT, FA, TCFA, or CA based on expert OCT readers, and as having high-lipid (HL), high-collagen (HC), or low-collagen/low-lipid (LCL) luminal composition based on linear discriminant analysis of FLIM. Of 47 plaques, 89.4% (42/47) of the plaques were correctly identified based on OCT/FLIM evaluation using tissue histopathology and immunohistochemistry as the gold standard. Four of the misclassifications corresponded to confusing PIT with HL luminal composition for FA with HL cap. The other corresponded to confusing FA with a HC cap for FA with an LCL cap.

Conclusion We have demonstrated the feasibility of accurate simultaneous OCT/FLIM morphological and biochemical characterization of coronary plaques at spatial resolutions and acquisition speeds compatible with catheter-based intravascular imaging. The success of this pilot study sets up future development of a multimodal intravascular imaging system that will enable studies that could help improve our understanding of plaque pathogenesis.

Keywords Atherosclerosis • Intravascular imaging • Vulnerable plaque • Optical coherence tomography • Fluorescence lifetime imaging

Introduction

Acute cardiovascular events are still the leading cause of morbidity and mortality in the Western world.[1–3] Invasive imaging of coronary atherosclerotic plaque is limited to the evaluation of its anatomical features and not to the evaluation of the metabolic processes, including inflammation,[4–7] oxidative stress, and dyslipidaemia, that lead to its development.[8,9] Early- and intermediate-stage atherosclerotic plaques have thin fibrous caps, lipid-laden cores, and localized inflammation that are inadequately visualized using optical coherence tomography (OCT) or intravascular ultrasound (IVUS) alone.[10,11] Convincing evidence exists to indicate that the underlying mechanisms in coronary plaque development leading to acute thrombosis are multifactorial, involving a complex interaction between structural, compositional, biomechanical, cellular, and molecular processes in the vessel wall.[12–14] Unfortunately, there is no current

* Corresponding author. Tel: +1 979 458 3335; Fax: +1 979 845 4450, E-mail: javierjo@tamu.edu

imaging modality (non-invasive or intravascular) that can provide such a level of plaque characterization. The future development of systemic or localized therapies for atherosclerosis likely will depend on a more detailed understanding of plaque development and progression after treatment.

Of the commercially available intravascular imaging tools, OCT provides the highest resolution images and can be used to define the superficial anatomical features of atherosclerotic plaque.[15–17] Endogenous fluorescence lifetime imaging (FLIM) enables the quantification of plaque's biochemical content near the luminal surface and the identification of lipid-rich and collagen-rich plaques.[18] Here, we examine the combination of OCT and FLIM to optically characterize plaque morphology and biochemical composition, and to compare the results to histopathology.

Methods

Imaging instrumentation

We have recently developed an integrated benchtop OCT and multispectral FLIM imaging system.[19] The OCT subsystem was based around a custom 53 kHz (maximum) line rate spectrometer and an 830 ± 20 nm SLED light source, providing an axial resolution of 7.6 μm in air and a 3 dB roll-off of ~1 mm. The FLIM subsystem was based on our previously published high-speed design.[20] A frequency tripled Q-switched Nd : YAG laser was used as the excitation source (355 nm, 30 kHz maximum repetition rate, 1 ns pulse full-width half maximum), and the fluorescence emission was separated into three bands (390 ± 20 nm for collagen, 452 ± 22.5 nm for elastin, and 550 ± 20 nm for lipids), which were detected with a micro channel plate-photo multiplier tube (rise time: 150 ps) and sampled with a high bandwidth digitizer (1.5 GHz, 4 GS/s).[20] The OCT and FLIM subsystems shared a common sample arm (common path), which featured an ultrabroadband achromatic objective lens, which provided an FLIM lateral resolution of 100 μm and an OCT lateral resolution of 14 μm.

Imaging protocol

Human coronary artery segments were obtained from eight autopsy cases within 48 h of death, according to a protocol approved by the Texas A&M University Institutional Review Board. A total of 47 arterial segments were longitudinally opened and imaged from the lumen side. The imaged field of view had an area of 2×2 mm^2. Immediately after imaging, each segment was ink-marked (for correlation with histopathology), fixed in 10% formalin, and sent for histopathological analysis.[21]

Histology

Three consecutive sections were cut every 500 μm to cover the whole length of each imaged arterial segment, and subsequently stained with Movat's pentachrome (for plaque histopathological classification), a mouse anti-human CD68 monoclonal antibody (for macrophage infiltration), or alpha-actin monoclonal antibody (for smooth muscle cells). All sections were evaluated by two cardiovascular pathologists (F.C. and L.M.B.), who agreed on the evaluation of all sections. On the basis of the histopathological evaluation,[14] each section was classified as pathological intimal thickening (PIT), fibroatheroma (FA), thin-cap FA (TCFA), or fibrocalcific plaque (CA). In addition, each plaque was classified based on the composition of the top 200 μm of luminal tissue (which corresponds to the estimated maximum penetration of the FLIM imaging) as having high-collagen (HC), high-lipid (HL), or low-collagen/low-lipid (LCL).

OCT plaque image evaluation

The OCT B-scans (cross-sectional images) were reviewed by two interventional cardiologists with clinical experience in the use of intravascular OCT (B.W. and M.F.) and one expert in intravascular OCT image processing (J.P.). Following standard criteria for intravascular OCT reading,[22] each plaque was classified as PIT, CA, FA, or TCFA. An FA was considered TCFA if the cap thickness was <80 μm.[22] When there was disagreement between the readers, the majority opinion was used. In all cases, at least two of the readers agreed on the classification.

FLIM plaque image evaluation

Following a methodology recently validated by our laboratory, the endogenous FLIM signal was analysed to classify the plaque luminal biochemical composition as HC, HL, or LCL.[18] The plaque autofluorescence was quantified in terms of the relative fluorescence intensity and the average lifetime at each pixel of the image. For statistical classification, multiclass Fisher's linear discriminant analysis was applied with the multispectral FLIM parameters (relative fluorescence intensity and average lifetime for each of spectral channel) as the feature vector for each pixel. A luminal biochemical map was then generated after classifying each pixel of an image to one of the three groups (HC, HL, or LCL). Finally, the entire plaque segments were assigned to one of the three groups as follows: if 20% or more of the pixels were classified as HL, the plaque was classified as HL; if <20% of the pixels were classified as HL, but at least 20% of the pixels were classified as HC, the plaque was classified as HC; if <20% of the pixels were classified as HL and <20% of the pixels were classified as HC, the plaque was classified as LCL.

Morphological and biochemical plaque characterization based on OCT and FLIM evaluation

To conduct an integrated OCT and FLIM plaque evaluation, the FLIM-derived biochemical map was superimposed on the surface of the OCT volumetric image (*Figures 2* and *3*, centre). It should be noted that while OCT (at 830 nm) can image up to ~1 mm deep into the tissue, the biochemical assessment offered by FLIM is integrated in depth and sensitive to the most superficial ~200 μm. The luminal biochemical map was colour-coded as LCL (blue), HC (green), or HL (red). Rendering the data as 2D cross-sectional images (*Figures 2* and *3*, left-top and right-top) is convenient for direct comparison with the histopathological sections (*Figures 2* and *3*, left-bottom and right-bottom). The resulting multimodal cross-sectional images (as in *Figures 1*, *4*, and *5*) were blindly reviewed by the two interventional cardiologists (B.W. and M.F.) and the expert in intravascular OCT image processing (J.P.).

Results

Histology

The histopathology evaluation of the 47 imaged coronary sections resulted in the following plaque distribution: PIT ($n = 26$), FA ($n = 12$), TCFA ($n = 2$), and CA ($n = 7$). Representative histology sections for each plaque type are shown in *Figure 1*. Plaque classification based on their luminal composition resulted in the following distribution: LCL ($n = 18$), HC ($n = 14$), and HL ($n = 15$).

OCT plaque image evaluation

Representative OCT B-scans for each plaque type are shown in *Figure 1*. A histopathological PIT plaque was characterized by a bright homogeneous single layer in OCT. An FA was identified by

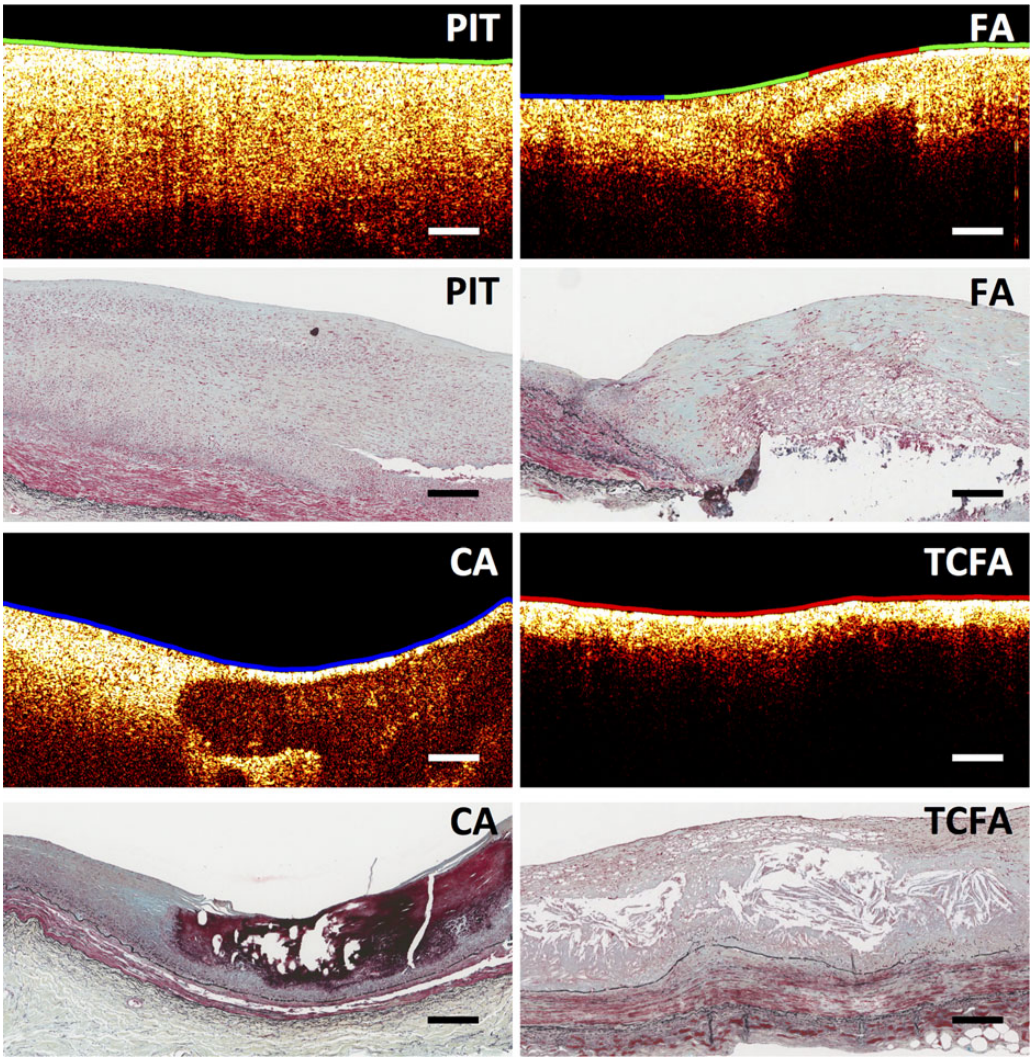

Figure 1 Sample B-scans and corresponding histopathology section (Movat stain) for each plaque type (PIT, FA, CA, and TCFA) as defined by the consensus standards for intravascular OCT.[22] The colour-coded lumen indicates the superficial plaque composition based on FLIM: HL as red, HC as green, and LCL as blue. All scale bars represent 200 μm.

OCT as having a signal-poor region showing diffuse borders corresponding to a necrotic core. A CA was identified by OCT as having a signal-poor region with well-defined sharp borders. A TCFA was identified by OCT as having a signal-poor region showing diffuse borders (necrotic core) covered by a thin bright layer of <80 μm (thin fibrous cap). All the FA (12 of 12), TCFA (2 of 2), and CA (7 of 7) plaques were correctly identified by OCT. Of the 26 PIT plaques, 21 were correctly classified and 5 were misclassified as FA.

FLIM plaque image evaluation

The FLIM-derived biochemical maps of all the histopathological LCL plaques showed <5% of HC or HL pixels; thus, they all (18 of 18) were correctly classified as LCL. The FLIM-derived biochemical maps of all the histopathological HL segments showed at least 25% of HL pixels; thus, they all (15 of 15) were correctly classified as HL. Of the 14 histopathological HC plaques, 13 were correctly classified as HC by FLIM and 1 was misclassified as LCL.

Morphological and biochemical plaque characterization

A sample fibrotic plaque with a mixed luminal composition is shown in *Figure 2*. An OCT B-scan (left-top) taken from the edge of the volume indicated a bright homogenous PIT plaque with LCL luminal composition, confirmed by histopathology (left-bottom). Another OCT B-scan (right-top) this time taken from the middle of the volume indicated a bright homogeneous PIT plaque with mixed HC (in the middle) and HL (at the sides) luminal composition, also confirmed by histopathology (right-bottom).

A sample CA with a mixed luminal composition is shown in *Figure 3*. An OCT B-scan (left-top) taken from the edge of the volume indicated a bright homogenous PIT plaque with HC luminal composition,

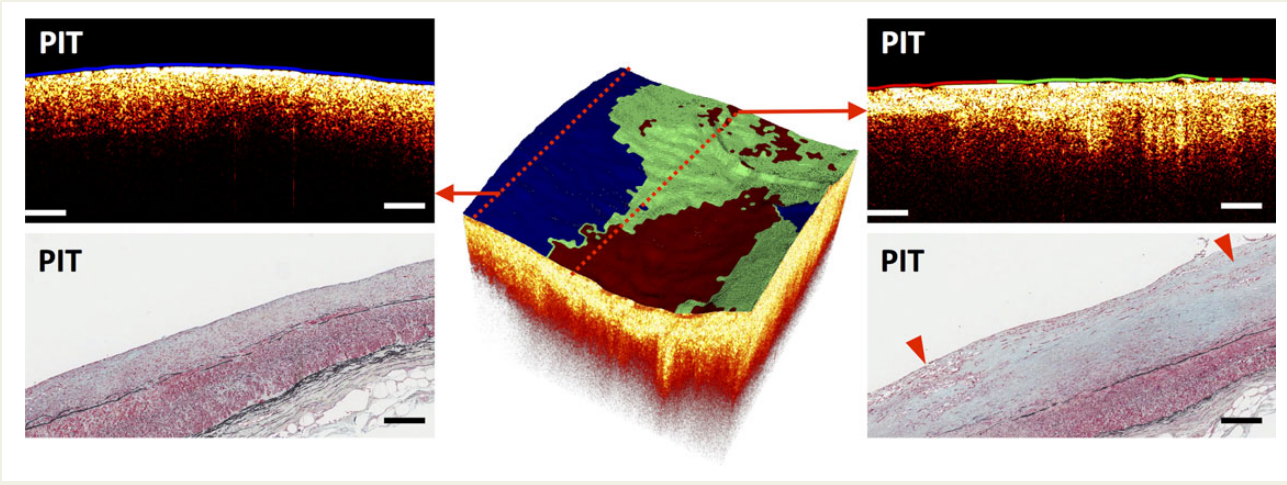

Figure 2 Sample multimodal OCT–FLIM volume of a fibrotic plaque with a mixed luminal biochemical composition. The colour-coded lumen indicates the superficial plaque composition based on FLIM: HL as red, HC as green, and LCL as blue. An OCT B-scan (left-top) taken from the edge of the volume indicated a PIT with an LCL (blue) superficial composition, confirmed by histopathology (left-bottom, Movat stain). Another OCT B-scan (right-top) taken from the middle of the volume indicated a PIT with mixed HC (green, middle) and HL (red, sides) superficial composition, also confirmed by histopathology (right-bottom, Movat stain). The red arrows on the histological section indicate areas with superficial macrophage/foam cell infiltration. All scale bars represent 200 μm.

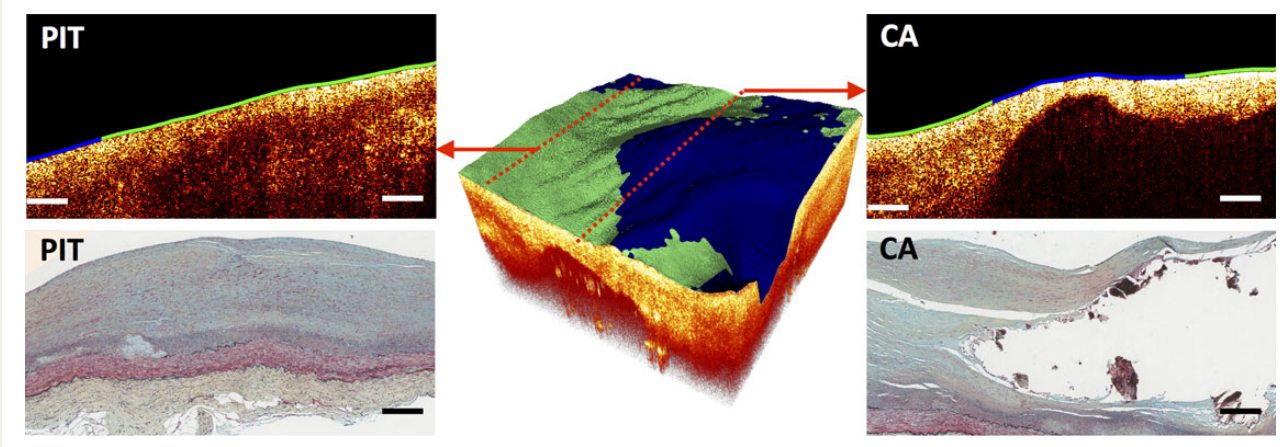

Figure 3 Sample multimodal OCT–FLIM volume of a CA with a mixed luminal biochemical composition. The colour-coded lumen indicates the superficial plaque composition based on FLIM: HL as red, HC as green, and LCL as blue. An OCT B-scan (left-top) taken from the edge of the volume indicated a PIT with a HC (green) superficial composition, confirmed by histopathology (left-bottom). Another OCT B-scan (right-top) taken from the middle of the volume showed a calcified necrotic core covered by a fibrous cap of mixed LCL (blue, middle) and HC (green, sides) composition, also confirmed by histopathology (right-bottom). All scale bars represent 200 μm.

confirmed by histopathology (left-bottom). Another OCT B-scan (right-top) this time taken from the middle of the volume showed a signal-poor region with well-defined sharp borders identified as a large calcified necrotic core covered by a fibrous cap of mixed LCL (in the middle) and HC (at the sides) composition, also confirmed by histopathology (bottom-right).

The multimodal plaque representation also enabled further characterization of PIT plaques based on their luminal composition. This is illustrated in *Figure 4*, in which three plaques were identified as PIT by OCT, but showed very distinct FLIM-based luminal biochemical maps that clearly distinguished HL, HC, and LCL histopathological compositions. While all three OCT B-scans were very similar showing uniform bright signal, the left plaque was identified by FLIM as having HL luminal composition, which was correlated with a significant macrophage foam cell infiltration in the top half of the plaque. The middle plaque was identified by FLIM as having HC luminal

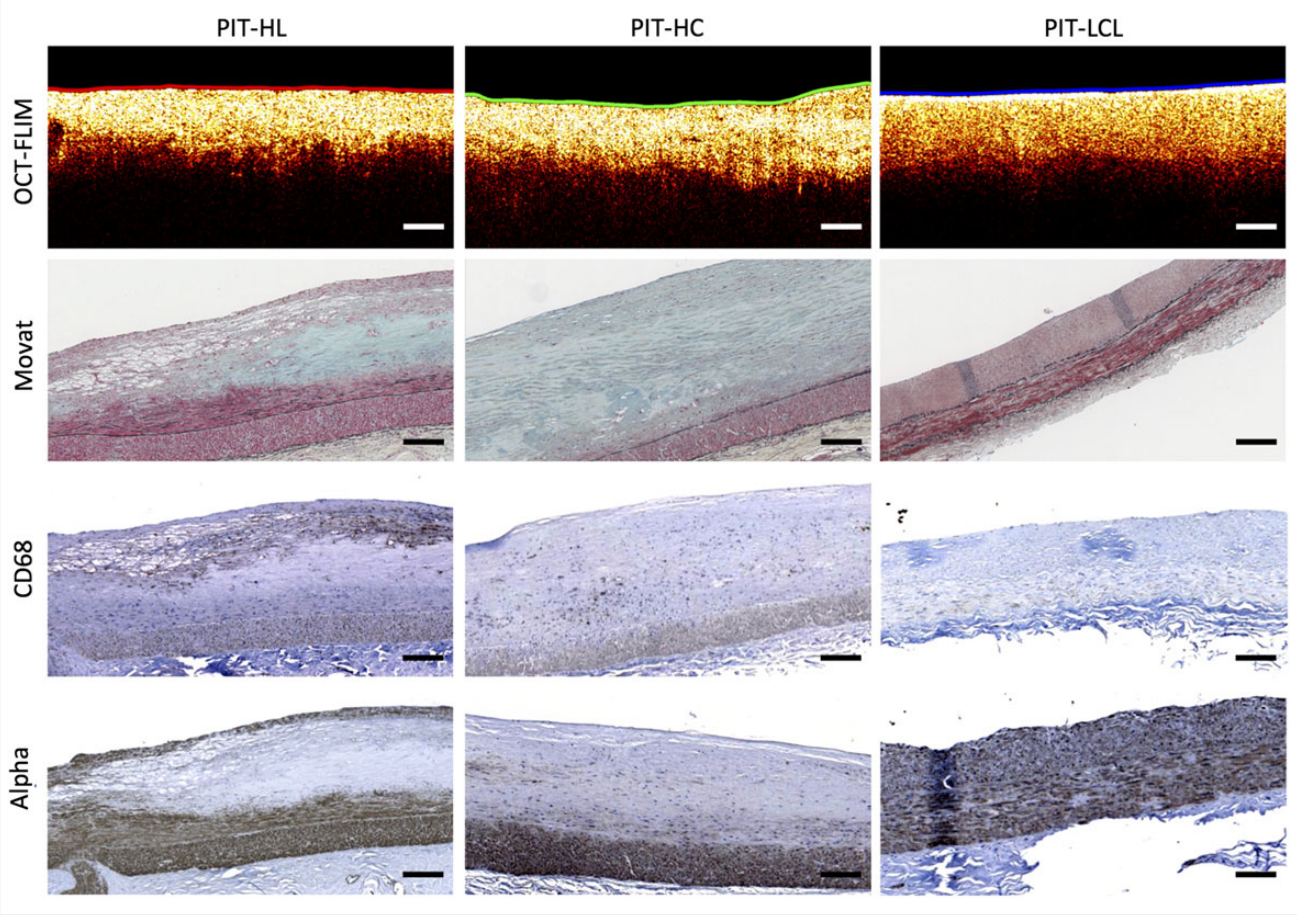

Figure 4 Sample PIT identified by OCT presenting a very distinct FLIM-derived luminal biochemical composition. The colour-coded lumen indicates the superficial plaque composition based on FLIM: HL as red, HC as green, and LCL as blue. First row: a multimodal OCT B-scan with the lumen colour-coded based on the FLIM-derived superficial composition. Second row: corresponding Movat-stained sections. Third row: corresponding CD68 sections for macrophage/foam cell identification. Fourth row: corresponding alpha-actin sections for smooth muscle cell identification. The left plaque was identified by FLIM as having a HL (red) superficial composition, which was correlated with a significant macrophage foam cell infiltration in the top half of the plaque. The middle plaque was identified by FLIM as having a HC (green) superficial composition, which was correlated with an almost exclusive collagen content. The right plaque was identified by FLIM as having an LCL (blue) superficial composition, which was correlated with a predominant smooth muscle cell composition and a lack of both macrophage foam cell infiltration and collagen. All scale bars represent 200 μm.

composition, which correlated with nearly exclusive collagen content. The right plaque was identified by FLIM as having LCL luminal composition, which was correlated with a predominant smooth muscle cell composition and a lack of both macrophage foam cell infiltration and collagen.

Similarly, this novel multimodal plaque representation also enabled a more detailed characterization of FA based on the cap biochemical composition. This is illustrated in *Figure 5*, in which two plaques were identified as FA by OCT, but showed very distinct FLIM-based biochemical maps. The left FA was identified by FLIM as having a HL cap, which was correlated with a significant macrophage foam cell infiltration throughout the fibrous cap. The right FA was identified by FLIM as having a HC cap, which was correlated with an almost exclusive collagen content with scattered smooth muscle cells.

As expected, two TCFAs identified by OCT showed a HL cap based on FLIM due to both macrophage foam cell infiltration of the thin fibrous cap and the close proximity of the necrotic core to the lumen, as shown in *Figure 1*. Finally, the CA could also be further characterized based on their luminal composition as shown in *Figure 3*.

Based on the described multimodal OCT/FLIM evaluation, each of the 47 imaged coronary segments was identified as PIT, FA, TCFA, or CA based on OCT, and as having LCL, HC, or HL luminal biochemical composition based on FLIM. Overall, 89.4% of the plaques (42/47) were correctly identified based on the multimodal OCT/FLIM evaluation. Four of the misclassifications corresponded to confusing PIT with HL luminal composition for FA with a HL cap. The other corresponded to confusing FA with a HC cap for FA with an LCL cap. The results of the multimodal OCT/FLIM evaluation are summarized in *Table 1*.

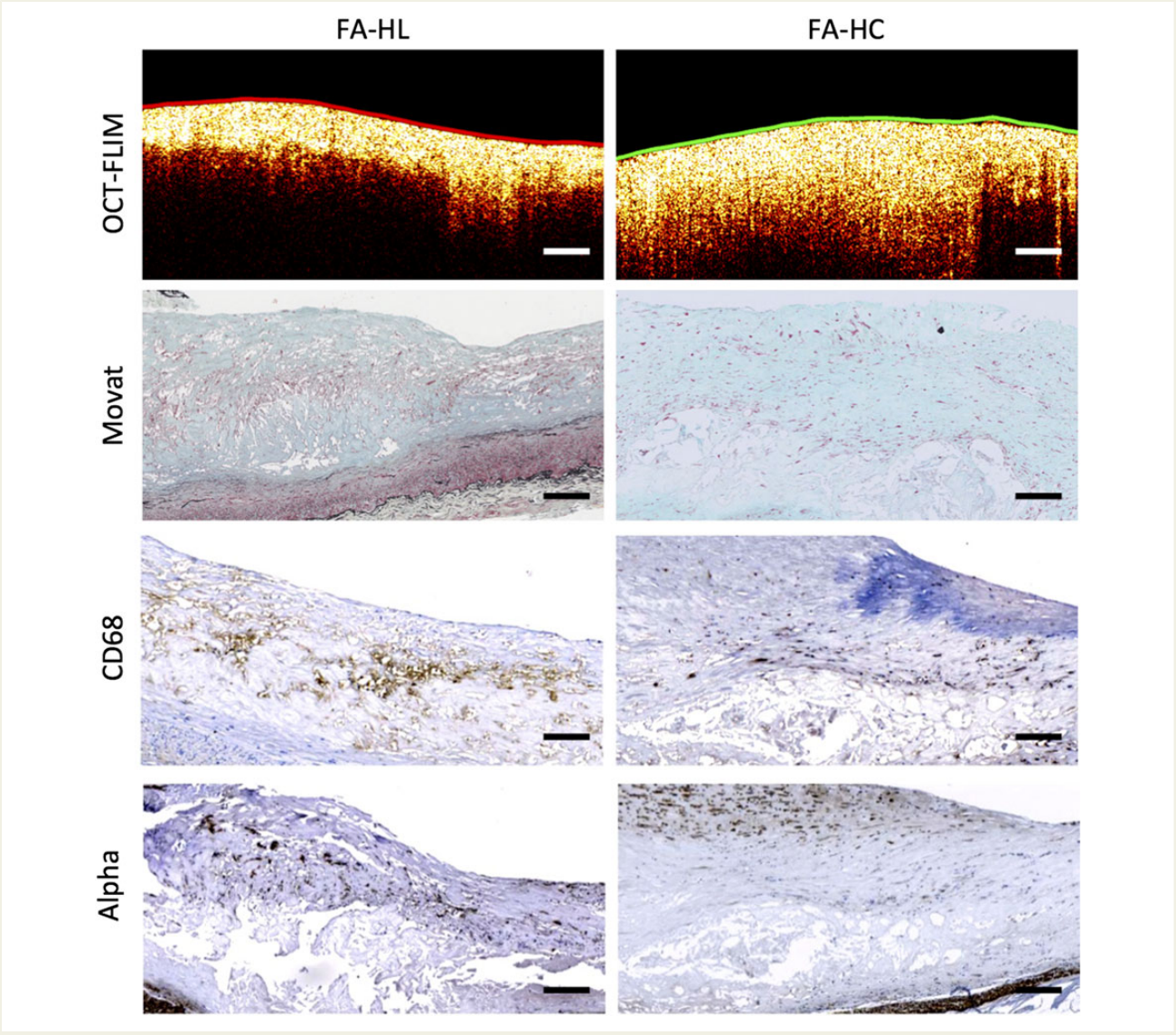

Figure 5 Sample FA identified by OCT presenting a very distinct FLIM-derived fibrous cap biochemical composition. The colour-coded lumen indicates the superficial plaque composition based on FLIM: HL as red, HC as green, and LCL as blue. First row: a multimodal OCT B-scan with the lumen colour-coded based on the FLIM-derived superficial composition. Second row: corresponding Movat-stained sections. Third row: corresponding CD68 sections for macrophage/foam cell identification. Fourth row: corresponding alpha-actin sections for smooth muscle cell identification. The left FA was identified by FLIM as having a HL (red) cap, which was correlated with a significant macrophage foam cell infiltration throughout the fibrous cap. The right FA was identified by FLIM as having a HC (green) cap, which was correlated with an almost exclusive collagen superficial composition and scattered smooth muscle cells. All scale bars represent 200 μm.

Discussion

In this study, we have demonstrated that simultaneous co-registered OCT and FLIM imaging of coronary plaques enables a detailed characterization of the plaque's morphology and lipid/collagen content. To our knowledge, this work represents the first attempt at integrating OCT-based morphological imaging with FLIM-based biochemical imaging for the purpose of atherosclerotic plaque characterization. Specifically, OCT is well suited to identifying layers, fibrous cap thickness, necrotic cores, and calcification, whereas endogenous FLIM enables the characterization of the luminal biochemical composition of the plaque, in particular its collagen and lipid content. Taken together, they enable the generation of detailed maps of plaque morphology and biochemistry.

Recently, a consensus has been reached on standard criteria to identify fibrous plaques, calcification, and necrotic/lipid pools in intravascular OCT cross-sectional images (B-scans).[22] In the present study, we have successfully applied these criteria to correctly identify all of the CA and TCFA plaques. However, the discrimination between PIT and FA was less effective, highlighting the difficulty in identifying necrotic cores or lipid pools by OCT evaluation, particularly when they are not superficial and when the cap is infiltrated by

Table I **Multimodal OCT/FLIM evaluation results**

	Multimodal OCT/FLIM evaluation							
	PIT-LCL	**PIT-HC**	**PIT-HL**	**FA-LCL**	**FA-HC**	**FA-HL**	**TCFA**	**CA**
PIT-LCL	13							
PIT-HC		4						
PIT-HL			5			**4**		
FA-LCL				1				
FA-HC				**1**	6			
FA-HL						4		
TCFA							2	
CA								7

Misclassifications are indicated as bold text.

macrophages, a limitation that was specifically highlighted in the consensus standards for intravascular OCT.[22] In the present study, this is further confounded by the fact that our OCT system is based at a centre wavelength of 830 nm, which has a more limited penetration depth than the typical 1300 nm centre wavelength used in commercial intravascular OCT systems.

The characterization of the lipid and collagen content of plaque is important for histopathological classification and for estimating the propensity of a plaque for developing into high-risk vulnerable plaque.[14] In the present study, endogenous FLIM was able to characterize the plaque luminal composition as being collagen rich, lipid rich, or collagen/lipid poor with almost 100% accuracy (one collagen-rich plaque was misclassified as collagen/lipid poor). A number of other imaging modalities have also been proposed for the identification of plaque composition.[13] Spectroscopic IVUS (the virtual histology technology developed by Volcano Corporation, San Diego, CA, USA) has shown some potential for detecting fibrotic and fibro-lipid plaque, but the technology's sensitivity and specificity have been questioned in several studies.[23–25] NIR spectroscopy (the intravascular platform developed by Infraredx, Inc., Burlington, MA, USA) provides accurate identification of lipid-rich plaques, but its capacity for assessing collagen content has not been demonstrated.[26] Our results, on the other hand, demonstrate that endogenous FLIM can be used not only for identifying lipid-rich plaques, but also for discriminating among fibrotic plaques rich in collagen (HC) from those with significant numbers of smooth muscle cells (LCL) (*Figure 4*). We believe that the additional information available through endogenous FLIM imaging represents a significant advantage over the other competing techniques.

We have previously provided evidence that the autofluorescence signal related to HL areas is related to the endogenous fluorescence emission of LDL.[18] Therefore, we believe that the presence of extracellular and intracellular LDL defines an HL area. Superficial significant (macrophage) foam cell infiltration will be detected as a HL area. However, since both extracellular and intracellular LDL can be present in plaques, a HL area could also be associated with a necrotic core, a lipid pool, foam cell infiltration, or any of their combinations. Therefore, FLIM alone will not allow identifying the actual histopathology of a HL area. The combination of FLIM and OCT, on the other hand, can provide a more complete histopathological assessment, by allowing identifying for instance a HL plaque as either an FA with a HL cap or a PIT with a HL luminal composition, as in *Figures 4* and *5*, respectively.

Although FLIM enables biochemical characterization of coronary plaques, little information about plaque morphology can be inferred from the autofluorescence signal. Only when the FLIM plaque classification was merged with the OCT scans was it possible to characterize plaque luminal biochemical composition and morphology simultaneously. In particular, the fibrous plaques correctly identified by OCT were further characterized as having significant collagen or lipid content based on the FLIM classification (*Figure 4*). Likewise, the FAs correctly identified by OCT were further characterized as having a fibrous cap rich in collagen or lipids (*Figure 5*).

While FLIM clearly provides valuable information on the biochemical composition of the tissues near the luminal surface, within the limited samples of this study it does not significantly improve the accuracy of the classification by the expert readers. When the OCT B-scans were reviewed independently by the three experts all of the FA, TCFA and CA were correctly identified. However, the discrimination of PIT was less effective: of 26, 5 PIT plaques with superficial macrophage/foam cell infiltration were misclassified as FA. When the OCT experts were asked to blindly review the B-scans of the five missed PIT plaques, this time with the FLIM-derived biochemical map indicating a HL, one plaque was correctly identified as PIT but the other four were again interpreted as an FA. Although the inclusion of the FLIM-derived biochemical map may have helped in one instance, a larger study incorporating additional training of the expert readers in how to utilize the FLIM information will be necessary to access the improvement, if any.

Some methods for automated intravascular OCT tissue characterization have been recently proposed. van Soest *et al.*[27] proposed an algorithm for the automatic quantification of the optical attenuation coefficient in intravascular OCT images, which allowed for discrimination of high attenuating plaque components (i.e. lipid core and macrophages infiltrations) from low attenuating components (i.e. fibrous and calcified tissue). Most recently, Ughi *et al.*[28] proposed a supervised classification approach combining the optical attenuation coefficient with texture features derived from intravascular OCT images for the identification of fibrous, calcific, and lipid-rich tissue. The local standard deviation of the intravascular OCT image has

also been proposed as an indication of macrophage infiltration in the fibrous cap of FAs.[29] Our multimodal optical imaging approach offers the unique opportunity to develop algorithms like those noted above for OCT imaging and to combine them with spectral signatures available from FLIM to generate automated algorithms based on the fusion of the OCT and FLIM information, thus providing more accurate plaque tissue characterization.

Other research groups have also recognized that fusing multiple imaging modalities to glean additional biomarkers may add a significant diagnostic value to the resulting images of atherosclerotic plaques. All of these approaches integrate IVUS with OCT, NIR spectroscopy, or fluorescence spectroscopy.[30,31] The integration of ultrasound and optical imaging, however, poses significant design challenges for the development of an appropriately sized intravascular catheter. Conversely, because both OCT and FLIM are optical imaging techniques, their integration into a single fiberoptic-based intravascular catheter poses fewer design issues. This is especially true in light of the continued commercial development of advanced fiberoptics that can accommodate the extremely broad spectral bandwidth (~350–1300 nm) required for a multimodal OCT–FLIM catheter.

Study limitations

Although our results clearly demonstrate the potential of simultaneous co-registered OCT and FLIM imaging for a more comprehensive characterization of coronary atherosclerotic plaques, this study was performed *ex vivo*, and it will be imperative to validate these results in intravascular *in vivo* conditions. We are in the midst of developing a system capable of such a study. In addition, we realize that the sample size of the present study was limited. Once the intravascular OCT/FLIM imaging system becomes available, it will be necessary to demonstrate the use of this multimodal optical technology for the identification of all histopathological types of coronary plaque in a larger *in vivo* study. The OCT system based at 830 nm used for this study has a more limited penetration depth than the typical intravascular OCT system based at 1300 nm. This limitation may have contributed to the confusion of FA for PIT and *vice versa* in the reading of the OCT images. Ongoing development of an intravascular OCT/FLIM system will obviate this issue by integrating a 1310 nm swept laser source-based OCT subsystem.

Conclusions

We have demonstrated the feasibility of accurate simultaneous OCT/FLIM morphological and biochemical characterization of coronary plaques at spatial resolutions and acquisition speeds compatible with catheter-based endoscopic imaging. We have shown that the integration of biochemical and morphological information enables a more complete characterization of atherosclerotic plaques. Moreover, endogenous FLIM enables the direct spectroscopic interrogation of the collagen and lipid content of the tissues near the luminal surface, which are important not only for histopathological classification but also for estimating the propensity of a plaque for developing into high-risk vulnerable plaque.[14] This pilot study provides the impetus for continued development of the combined OCT and FLIM system for intravascular multimodal imaging.

Conflict of interest: None declared.

Funding

This study was supported by the American Heart Association (beginning grant-in-aid grant 0765102Y) and the National Institutes of Health (NIH; 1R21CA132433 and 1R01HL11136).

References

1. Gillum RF. Trends in acute myocardial infarction and coronary heart disease death in the United States. *J Am Coll Cardiol* 1994;**23**:1273–7.
2. Ounpuu S, Negassa A, Yusuf S. INTER-HEART: a global study of risk factors for acute myocardial infarction. *Am Heart J* 2001;**141**:711–21.
3. Yusuf S, Reddy S, Ounpuu S, Anand S. Global burden of cardiovascular diseases: part II: variations in cardiovascular disease by specific ethnic groups and geographic regions and prevention strategies. *Circulation* 2001;**104**:2855–64.
4. Fuster V, Fayad ZA, Moreno PR, Poon M, Corti R, Badimon JJ. Atherothrombosis and high-risk plaque: part II: approaches by noninvasive computed tomographic/magnetic resonance imaging. *J Am Coll Cardiol* 2005;**46**:1209–18.
5. Granada JF, Kaluza GL, Raizner AE, Moreno PR. Vulnerable plaque paradigm: prediction of future clinical events based on a morphological definition. *Catheter Cardiovasc Interv* 2004;**62**:364–74.
6. Jefferson BK, Topol EJ. Molecular mechanisms of myocardial infarction. *Curr Probl Cardiol* 2005;**30**:333–74.
7. Ross R. Atherosclerosis is an inflammatory disease. *Am Heart J* 1999;**138**(5 Pt 2): S419–20.
8. Quinn MT, Parthasarathy S, Fong LG, Steinberg D. Oxidatively modified low density lipoproteins: a potential role in recruitment and retention of monocyte/macrophages during atherogenesis. *Proc Natl Acad Sci USA* 1987;**84**:2995–8.
9. Stocker R, Keaney JF Jr. Role of oxidative modifications in atherosclerosis. *Physiol Rev* 2004;**84**:1381–478.
10. Libby P. Inflammation in atherosclerosis. *Nature* 2002;**420**:868–74.
11. Naghavi M, Libby P, Falk E, Casscells SW, Litovsky S, Rumberger J *et al.* From vulnerable plaque to vulnerable patient: a call for new definitions and risk assessment strategies: part II. *Circulation* 2003;**108**:1772–8.
12. Alfonso F, Virmani R. New morphological insights on coronary plaque rupture: bridging the gap from anatomy to clinical presentation? *JACC Cardiovasc Interv* 2011;**4**:83–6.
13. Finn AV, Nakano M, Narula J, Kolodgie FD, Virmani R. Concept of vulnerable/unstable plaque. *Arterioscler Thromb Vasc Biol* 2010;**30**:1282–92.
14. Virmani R, Burke AP, Farb A, Kolodgie FD. Pathology of the vulnerable plaque. *J Am Coll Cardiol* 2006;**47**(8 Suppl:C13–8.
15. Jang I-K, Tearney GJ, MacNeill B, Takano M, Moselewski F, Iftima N *et al.* In vivo characterization of coronary atherosclerotic plaque by use of optical coherence tomography. *Circulation* 2005;**111**:1551–5.
16. MacNeill BD, Bouma BE, Yabushita H, Jang IK, Tearney GJ. Intravascular optical coherence tomography: cellular imaging. *J Nucl Cardiol* 2005;**12**:460–5.
17. Yabushita H, Bouma BE, Houser SL, Aretz HT, Jang I-K, Schlendorf KH *et al.* Characterization of human atherosclerosis by optical coherence tomography. *Circulation* 2002;**106**:1640–5.
18. Park J, Pande P, Shrestha S, Clubb F, Applegate BE, Jo JA. Biochemical characterization of atherosclerotic plaques by endogenous multispectral fluorescence lifetime imaging microscopy. *Atherosclerosis* 2012;**220**:394–401.
19. Park J, Jo JA, Shrestha S, Pande P, Wan Q, Applegate BE. A dual-modality optical coherence tomography and fluorescence lifetime imaging microscopy system for simultaneous morphological and biochemical tissue characterization. *Biomed Opt Express* 2010;**1**:186–200.
20. Shrestha S, Applegate BE, Park J, Xiao X, Pande P, Jo JA. High-speed multispectral fluorescence lifetime imaging implementation for in vivo applications. *Opt Lett* 2010;**35**:2558–60.
21. Newby AC, Zaltsman AB. Fibrous cap formation or destruction—the critical importance of vascular smooth muscle cell proliferation, migration and matrix formation. *Cardiovasc Res* 1999;**41**:345–60.
22. Tearney GJ, Regar E, Akasaka T, Adriaenssens T, Barlis P, Bezerra HG *et al.* Consensus standards for acquisition, measurement, and reporting of intravascular optical coherence tomography studies: a report from the International Working Group for Intravascular Optical Coherence Tomography Standardization and Validation. *J Am Coll Cardiol* 2012;**59**:1058–72.
23. Nakazawa G, Finn AV, Virmani R. Virtual histology: does it add anything? *Heart* 2007; **93**:897–8.
24. Sawada T, Shite J, Garcia-Garcia HM, Shinke T, Watanabe S, Otake H *et al.* Feasibility of combined use of intravascular ultrasound radiofrequency data analysis and optical coherence tomography for detecting thin-cap fibroatheroma. *Eur Heart J* 2008;**29**: 1136–46.

25. Thim T, Hagensen MK, Wallace-Bradley D, Granada JF, Kaluza GL, Drouet L *et al.* Unreliable assessment of necrotic core by virtual histology intravascular ultrasound in porcine coronary artery disease/clinical perspective. *Circ Cardiovasc Imaging* 2010; **3**:384–91.
26. Waxman S, Dixon SR, L'Allier P, Moses JW, Petersen JL, Cutlip D *et al.* In vivo validation of a catheter-based near-infrared spectroscopy system for detection of lipid core coronary plaques: initial results of the SPECTACL study. *J Am Coll Cardiol Imaging* 2009;**2**:858–68.
27. van Soest G, Regar E, Goderie TPM, Gonzalo N, Koljenovic S, van Leenders GJLH *et al.* Pitfalls in plaque characterization by OCT: image artifacts in native coronary arteries. *J Am Coll Cardiol Imaging* 2011;**4**:810–3.
28. Ughi GJ, Adriaenssens T, Sinnaeve P, Desmet W, D'hooge J. Automated tissue characterization of in vivo atherosclerotic plaques by intravascular optical coherence tomography images. *Biomed Opt Express* 2013;**4**:1014–30.
29. Tearney GJ, Yabushita H, Houser SL, Aretz HT, Jang IK, Schlendorf KH *et al.* Quantification of macrophage content in atherosclerotic plaques by optical coherence tomography. *Circulation* 2003;**107**:113–9.
30. O'Donnell M, McVeigh ER, Strauss HW, Tanaka A, Bouma BE, Tearney GJ *et al.* Multimodality cardiovascular molecular imaging technology. *J Nucl Med* 2010;**51**(Suppl 1):38S–50.
31. Sun Y, Chaudhari AJ, Lam M, Xie H, Yankelevich DR, Phipps J *et al.* Multimodal characterization of compositional, structural and functional features of human atherosclerotic plaques. *Biomed Opt Express* 2011;**2**:2288–98.

IMAGE FOCUS

doi:10.1093/ehjci/jev122
Online publish-ahead-of-print 30 April 2015

An auscultatory conundrum: severe mitral stenosis with a third heart sound?

William R. Miranda, Darrell B. Newman, Jeffrey B. Geske, and Rick A. Nishimura*

Division of Cardiovascular Diseases, Mayo Clinic, 200 First Street SW, Rochester, MN 55905, USA

* Corresponding author. Tel: +1 507 774 2129; Fax: +1 507 538 6915, E-mail: rnishimura@mayo.edu

A 70-year-old asymptomatic woman was referred for intervention of severe mitral stenosis (MS). Physical exam demonstrated a soft first and normally split second heart sound, an apical 2/6 holosystolic murmur and a soft diastolic rumble. There was also a loud early diastolic filling sound—S3 (sound clip, Supplementary data online) (*Panel C*). Transthoracic echocardiography revealed normal left ventricular size and function (ejection fraction 72%) and an estimated right ventricular systolic pressure of 69 mmHg. There was severe mitral annular calcification (*Panel A*) with associated restricted leaflet motion. The diagnosis of severe MS was made with a continuous wave Doppler transmitral mean gradient of 11 mmHg (heart rate 59 bpm). Mild–moderate mitral regurgitation (MR) was identified by a small color flow jet into the left atrium (*Panel B*). Given the discrepancy between auscultatory findings and the echocardiographic interpretation, transoesophageal echocardiography was performed, demonstrating moderate-to-severe MR (*Panel D*)—regurgitant volume of 51 mL by proximal isovolumic surface area. Thus, mitral balloon valvotomy was not recommended.

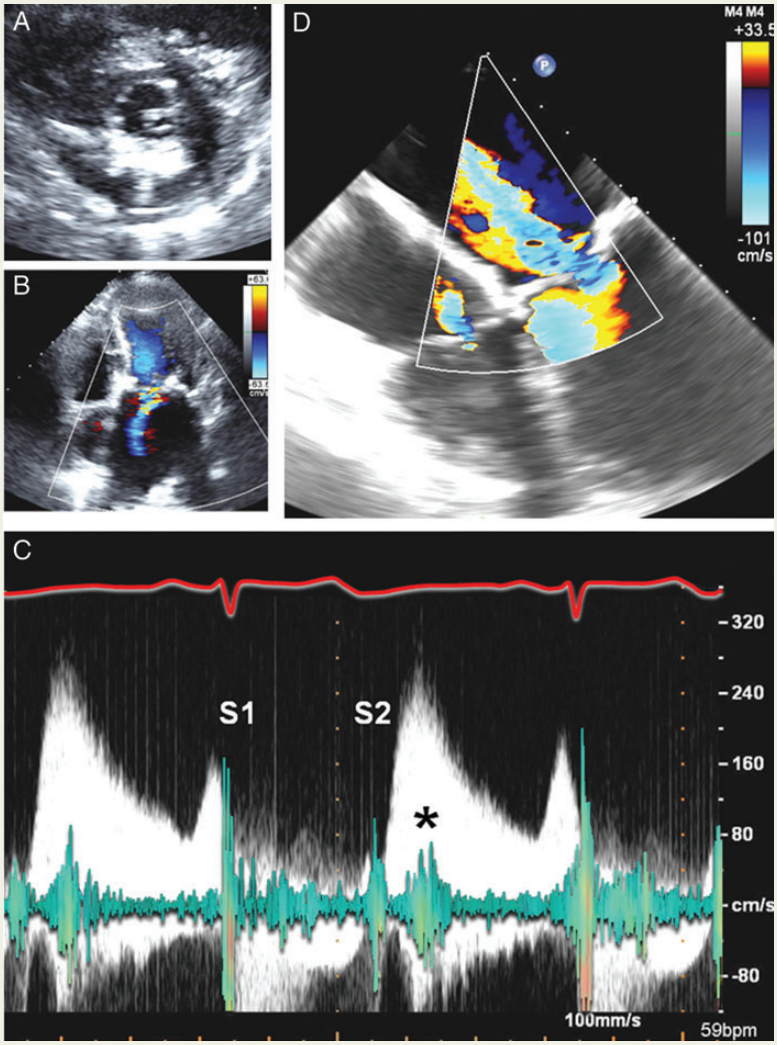

Our case underscores the importance of physical examination in the evaluation of valvular heart disease—severe isolated MS and an S3 should not coexist. Acoustic shadowing in the setting of extensive mitral annular calcification may result in underestimation of MR severity by color Doppler. A large V wave from significant MR results in a high driving pressure, which may be misinterpreted as true obstruction. Under appreciation of MR should be suspected if an S3 is auscultated, which correlates with a high E wave velocity and markedly elevated *E/A* ratio on transmitral Doppler interrogation.

Supplementary data are available at *European Heart Journal – Cardiovascular Imaging* online.